APPLYING MACHINE LEARNING TO LONGITUDINAL PHASE SPACE RECONSTRUCTION IN THE LANSCE CCL*

M. J. Kay†, P. M. Anisimov, C. A. Leon
Los Alamos National Laboratory, Los Alamos, United States

Abstract

Traditional phase scans at LANSCE are useful for tuning longitudinal capture but provide only indirect information about the bunch distribution. This work extends a deep neural network-based reconstruction method to the first two modules of the side-coupled cavity linac. Simulated two-dimensional phase scans were generated with HPSim by varying the RF phases of Modules 5 and 6 and recording the transmitted current after the absorber/collector diagnostic. A retrained network reconstructed correlated Gaussian longitudinal phase space distributions from these scans, recovering their approximate size, orientation, and centroid. These results support further development using realistic distributions and measured CCL phase scans.

INTRODUCTION

The Los Alamos Neutron Science Center (LANSCE) linear accelerator accelerates an H^- beam from 750 keV to 100 MeV in a 201.25-MHz drift tube linac (DTL), and then from 100 MeV to 800 MeV in an 805-MHz side-coupled cavity linac (CCL). Tuning each section of the linac traditionally relies on analyzing empirical observables derived from a sequence of phase scan measurements to verify proper longitudinal capture [1,2]. Although these scans are effective for minimizing beam loss, they provide only indirect information about the longitudinal beam distribution and may obscure features such as distorted bunch shapes or multiple beam cores. To address this limitation, a new method of extracting the longitudinal beam distribution from phase scans has been proposed. This method uses a deep neural network (DNN) to reconstruct the beam distribution from a two-dimensional phase scan (TDPS). This approach was recently demonstrated for the LANSCE DTL using training data generated with the High-Performance Simulator (HPSim) [3,4], where the input beam distribution at the entrance to DTL Module 1 was reconstructed from TDPS data for Modules 1 and 2 [5].

This paper applies the same approach to the first two modules of the LANSCE CCL, Modules 5 and 6. These modules are equipped with an absorber/collector diagnostic similar to that used for DTL phase scans, simplifying the translation of the method to the CCL. As an initial validation, HPSim was used to generate TDPS data for correlated Gaussian input distributions, and a DNN was retrained to reconstruct the longitudinal phase space at the entrance to Module 5. This paper introduces the CCL TDPS, describes its interpretation in terms of longitudinal acceptance, and presents preliminary reconstruction results using synthetic data.

* The research presented in this article was supported by the Laboratory Directed Research and Development program of Los Alamos National Laboratory under project number 20250783MFR.
† mkay@lanl.gov

TWO-DIMENSIONAL PHASE SCANS FOR CCL MODULES 5 AND 6

A TDPS is performed by varying the RF phases of two consecutive linac modules while measuring the transmitted beam current at the output. For CCL Modules 5 and 6, this measurement uses the absorber/collector diagnostic located downstream of Module 6. The absorber acts as an energy filter, stopping H^- ions below 121 MeV (96% of the design energy after Module 6), while ions above this threshold are stopped in the collector. The current read from the collector is proportional to the number of H^- ions stopped in the collector and is therefore used as the transmission signal.

By scanning the phases of Modules 5 and 6, the longitudinal acceptance of the CCL is systematically modified. The TDPS produces a map of collector current as a function of the Module 5 phase, ϕ_5, and the relative phase between Modules 6 and 5, $\phi_{65} = \phi_6 - \phi_5$. Figure 1 shows the result of a TDPS simulated in HPSim, in which both ϕ_5 and ϕ_{65} were scanned over 360°. The broad high-current region indicates there is a range of phase settings that provide efficient longitudinal capture. In this simulation, the maximum transmission occurs at $\phi_5 = -137°$ and $\phi_{65} = 90°$.

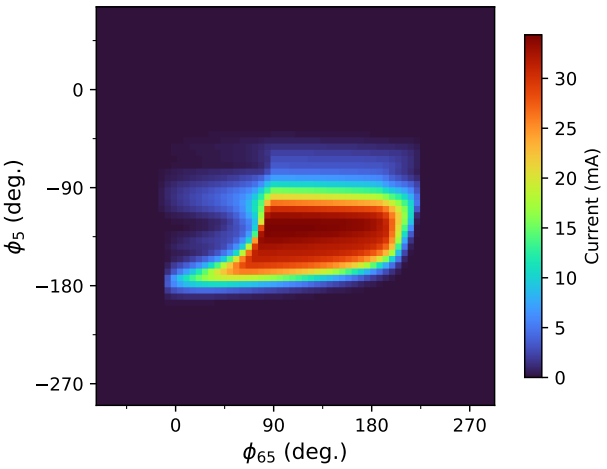

Figure 1: Simulated TDPS for CCL Modules 5 and 6.

The collector current gives a scalar measure of how well the longitudinal acceptance function overlaps with the bunch in phase space. For each phase setting $j = (\phi_5, \phi_{65})$, the CCL and absorber/collector system define an effective longitudinal acceptance function $A_j(\phi, w)$. The collector current

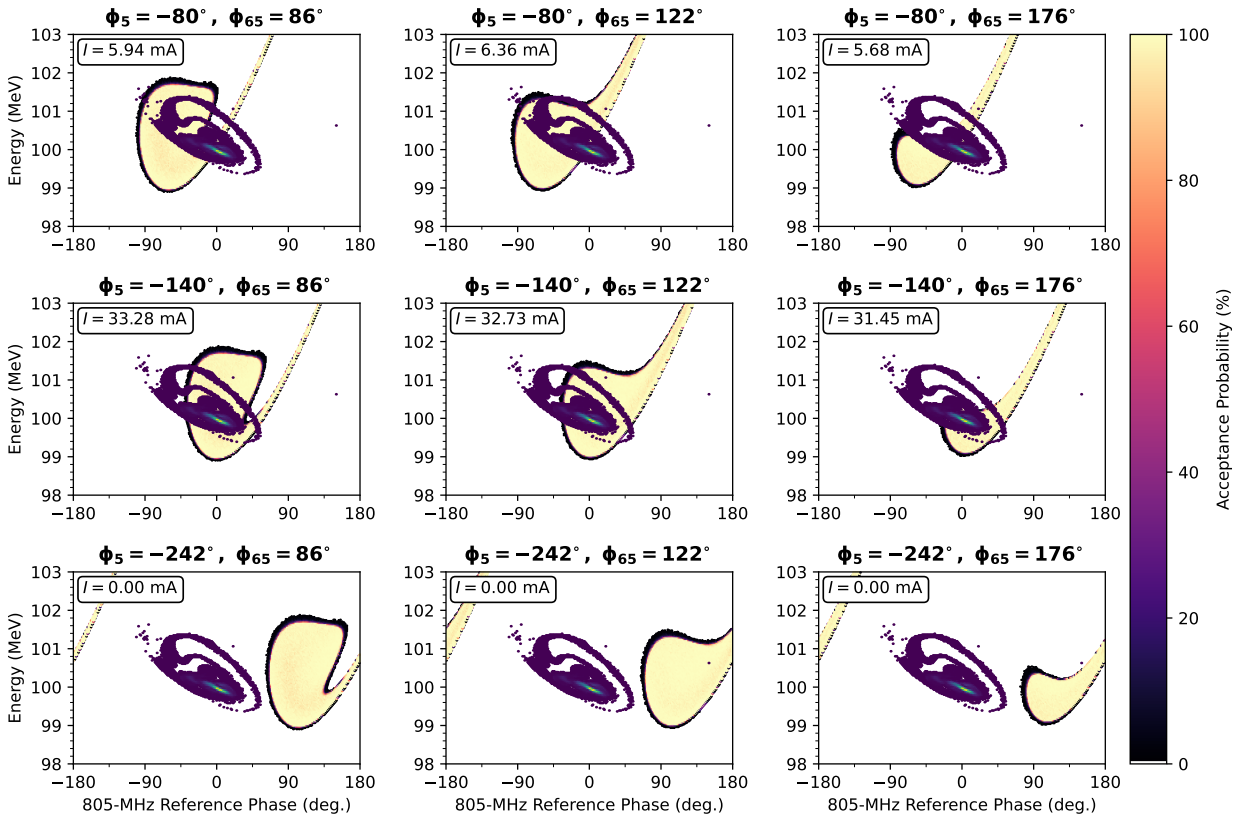

Figure 2: Overlap of the acceptance function and H^- bunch for different combinations of ϕ_5 and ϕ_{65}.

for each phase combination is given analytically by an overlap integral between that acceptance and the unknown beam distribution,

$$I_j = \iint A_j(\phi, w) f(\phi, w)\, d\phi\, dw, \qquad (1)$$

where $f(\phi, w)$ is the beam current density, and ϕ and w are the phase and energy coordinates, respectively.

The features in the TDPS in Fig. 1 can be understood by considering how ϕ_5 and ϕ_{65} modify the longitudinal acceptance function. Figure 2 shows how the acceptance function overlaps with the input beam for a number of (ϕ_5,ϕ_{65}) combinations. Each row in Fig. 2 corresponds to a different value of ϕ_5, and each column corresponds to a different value of ϕ_{65}. It can be seen that the two phase variables have distinct effects: changing ϕ_5 shifts the acceptance function along the phase axis, while changing ϕ_{65} modifies its shape and area. Near $\phi_{65} = 90°$, the acceptance function contains a relatively large region with nearly 100% transmission probability, bounded by regions where the acceptance rapidly falls to zero. The high-current region in Fig. 1 therefore corresponds to phase settings for which the main beam core lies within the high-acceptance region. The sloped edges of this region occur when the beam core is only partially accepted, such as shown in the top row of Fig. 2. Conversely, the near-zero-current regions occur when the beam core lies outside the accepted region, as illustrated in the bottom row of Fig. 2.

PRELIMINARY RESULTS

Initial testing of the DNN-based reconstruction method was performed using synthetic data generated with HPSim. This study was intended as a controlled validation of the CCL reconstruction workflow rather than a final demonstration on realistic beam distributions. Because the TDPS response in the CCL has the same basic structure as in the DTL, namely translation of the acceptance in phase and variation of the acceptance shape, the DNN approach previously developed for the DTL was adapted and retrained for the CCL. Details of the model architecture are given in [5].

The DNN input was a simulated 32×32 TDPS map, such as the one shown in Fig. 1, and the target output was a 2-D histogram of the longitudinal phase space distribution of the bunch at the entrance to Module 5. A preliminary data set of 741 input/output pairs was used for retraining. Each case was generated from an input beam containing 10^6 macroparticles. To simplify model validation, the longitudinal distribution was replaced by a correlated 2-D Gaussian centered at $(0.0°, 100.0\ \text{MeV})$, while the original transverse distribution was retained. The Gaussian parameters were randomly sampled from uniform distributions with $\sigma_\phi \in [10.0, 25.0)$ degrees, $\sigma_w \in [0.1, 0.5)$ MeV, and $\rho \in [-1, 1)$. The primary loss function was the mean squared error between the true and predicted 2-D longitudinal phase space histograms.

Figure 3 shows example reconstructions for three input beams. The top row shows the true distributions, and the bottom row shows the corresponding DNN predictions inferred

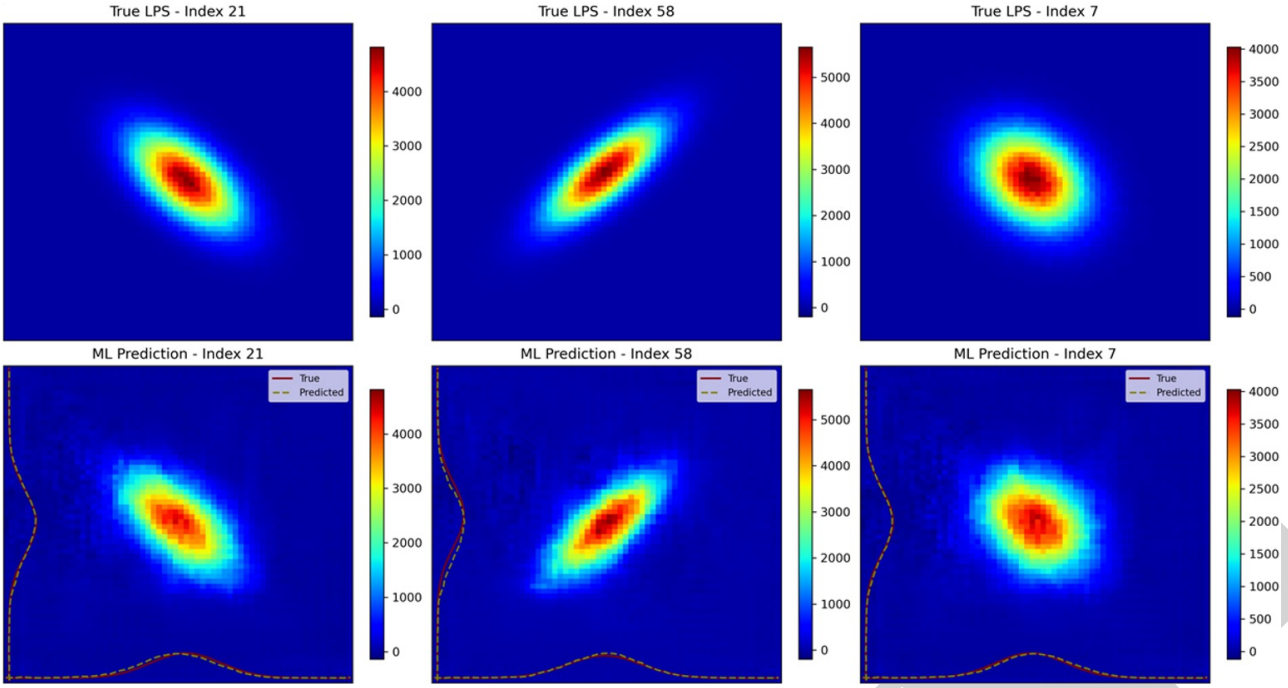

Figure 3: Example DNN reconstructions of correlated Gaussian input beam distributions from simulated TDPS data.

from the simulated TDPS data. The model recovers the approximate size, orientation, and centroid of the Gaussian beam distributions, demonstrating that the TDPS contains sufficient information for reconstruction in this simplified case. Some residual smoothing and low-amplitude artifacts are visible in the predicted distributions, indicating that further training and validation are needed. Future work will increase the size and diversity of the training set and extend the method to more realistic, non-Gaussian beam distributions before applying it to measured CCL phase scans.

CONCLUSION

A machine learning-driven tomographic reconstruction technique for longitudinal beam phase space characterization has been investigated for application to the first two modules of the LANSCE CCL. By performing two-dimensional scans of the RF phases in Modules 5 and 6, the longitudinal acceptance of the accelerator can be systematically modified, producing transmission measurements that encode information about the input beam distribution. Simulations performed with HPSim show that the two phase parameters have largely distinct effects on the longitudinal acceptance, enabling effective sampling of longitudinal phase space. A deep neural network trained on synthetic TDPS data successfully reconstructed correlated Gaussian beam distributions with reasonable fidelity, demonstrating the feasibility of the approach. These preliminary results provide a strong foundation for extending the method to more realistic beam distributions and ultimately to experimental measurements on the operating accelerator. Successful deployment of this technique would provide a powerful new diagnostic capability for longitudinal beam tuning and optimization at LANSCE.

ACKNOWLEDGMENTS

This research used resources provided by the Los Alamos National Laboratory Institutional Computing Program, which is supported by the U.S. Department of Energy National Nuclear Security Administration under Contract No. 89233218CNA000001.

REFERENCES

[1] Longitudinal Tuning of the LAMPF 201.25-MHz Linac Without Space Charge, Los Alamos Scientific Laboratory, Los Alamos, NM, USA, Rep. LA-6863, Mar. 1978. doi:10.2172/5068593

[2] The Δt Tuneup Procedure for the LAMPF 805-MHz Linac, Los Alamos Scientific Laboratory, Los Alamos, NM, USA, Rep. LA-6374-MS, Jun. 1976. https://www.osti.gov/servlets/purl/7353211

[3] X. Pang and L. Rybarcyk, "GPU accelerated online multi-particle beam dynamics simulator for ion linear particle accelerators", *Comp. Phys. Comm.*, vol. 185, no. 3, pp. 744-753, 2014. doi:10.1016/j.cpc.2013.10.033

[4] E.-C. Huang, P.M. Anisimov and L.J. Rybarcyk, "Benchmarking HPSim with the LANSCE linac", in *Proc. IPAC'23*, Venice, Italy, May 2023, pp. 2480-2482. doi:10.18429/JACoW-IPAC2023-TUPM112

[5] P.M. Anisimov, E.-C. Huang and A. Scheinker, "Machine learning-driven longitudinal phase space reconstruction for enhanced beam tuning at LANSCE", in *Proc. IPAC'25*, Taipei, Taiwan, June 2025, pp. 2733-2736. doi:10.18429/JACoW-IPAC2025-THPM024